PFC-JA-81-8

FREE ELECTRON LASER INSTABILITY FOR A RELATIVISTIC SOLID ELECTRON BEAM IN A HELICAL WIGGLER FIELD

H. S. Uhm
R. C. Davidson

4/81

FREE ELECTRON LASER INSTABILITY FOR A RELATIVISTIC SOLID ELECTRON BEAM IN A HELICAL WIGGLER FIELD

Han S. Uhm
Naval Surface Weapons Center
White Oak, Silver Spring, Maryland 20910

Ronald C. Davidson
Plasma Fusion Center
Massachusetts Institute of Technology
Cambridge, Massachusetts 02139

and

Science Applications, Inc.
Boulder, Colorado 80302

The free electron laser instability for a solid relativistic electron beam propagating in combined transverse helical wiggler and uniform axial guide fields is investigated within the framework of the linearized Vlasov-Maxwell equations. It is assumed that $\nu/\gamma_b \ll 1$, where ν is Budker's parameter and $\gamma_b mc^2$ is the electron energy. Stability properties are investigated for the choice of equilibrium distribution function in which all electrons have the same value of the linear combination of transverse and helical invariants, $C_\perp - 2\gamma_b m\omega_b C_h =$ const., and a Lorentzian distribution in the axial invariant C_z. (Here ω_b is a constant.) The instability growth rate is calculated including a determination of the optimum value of the ratio of beam radius to conducting wall radius (R_0/R_c) for maximum growth. It is found that the maximum growth rate for a solid electron beam is comparable to that for a hollow beam with similar parameters. Moreover, the introduction of a small axial momentum spread ($\Delta/\gamma_b mc \lesssim$ a few percent) significantly reduces the instability growth rate.

I. INTRODUCTION

In recent years, the free electron laser instability[1-9] has been extensively investigated with particular emphasis on applications to intense microwave generation. For the most part, previous theoretical analyses of this instability have been carried out either for uniform density beams[3-6] with infinite transverse dimension, or for annular electron beams.[7,8] The present paper examines the influence of finite radial geometry on the free electron laser instability for a solid electron beam propagating in combined transverse helical wiggler and uniform axial guide fields. The analysis is carried out within the framework of the linearized Vlasov-Maxwell equations, including a determination of the optimum value of beam radius R_0 for maximum growth rate.

The present analysis is carried out for an infinitely long relativistic electron beam propagating in the combined transverse wiggler and uniform axial guide fields described by Eq. (1). Equilibrium and stability properties are calculated for the specific choice of electron distribution function [Eq. (5)],

$$f_b^0 = \frac{n_0}{\pi}\,\delta(C_\perp - 2\gamma_b m\omega_b C_h - 2\gamma_b m\hat{T}_\perp)G(C_z) \ ,$$

where n_0, ω_b, γ_b, and $\hat{T}_\perp$ are positive constants, $C_\perp$, C_h, and C_z are the transverse, helical, and axial invariants[10] defined in Eqs. (6) - (8), and the axial distribution function is normalized according to $\int_{-\infty}^{\infty} dC_z G(C_z) = 1$. Equilibrium properties are investigated in Sec. II, and stability properties are examined in Secs. III and IV, assuming that $\nu/\gamma_b \ll 1$, where ν is Budker's parameter, $\gamma_b mc^2$ is the characteristic electron energy, and m is the electron rest mass.

In Sec. III, making use of the linearized Vlasov-Maxwell equations, we obtain the coupled eigenvalue equations (33), (37), (40), (45), and (46) that describe free electron laser stability properties in circumstances where the perturbed transverse fields can be approximated by the vacuum waveguide fields. For short wavelength perturbations, the axial component of the perturbed longitudinal field can be approximated by [Eq. (49)],

$$\hat{E}^{(n)}_{z,\ell}(r) = \begin{cases} \hat{\phi}_{\ell,s'} J_\ell(\beta_{\ell,s'} r/R_0) , & 0 \leq r < R_0 , \\ 0 , & \text{otherwise} , \end{cases}$$

where $J_\ell(x)$ is the Bessel function of the first kind of order ℓ, $\beta_{\ell,s'}$ is the s'th zero of $J_\ell(\beta_{\ell,s'}) = 0$ and $\hat{\phi}_{\ell,s'}$ is a constant. In Sec. IV, substituting Eq. (49) into the coupled eigenvalue equations, we obtain closed algebraic dispersion relations for the transverse electric (TE) and transverse magnetic (TM) polarizations.

Introducing the normalized dimensionless function [Eq. (59)],

$$G_{\ell s'}(x) = 4\beta^2_{\ell,s'} \frac{J^2_\ell(x)}{(x^2 - \beta^2_{\ell,s'})^2} ,$$

it is shown in Sec. IV that the coupling between the longitudinal and transverse perturbations is proportional to $G_{\ell s'}(\alpha_{\ell+1,s} R_0/R_c)$ for the TE mode, and to $G_{\ell s'}(\beta_{\ell+1,s} R_0/R_c)$ for the TM mode. Here $\alpha_{\ell+1,s}$ and $\beta_{\ell+1,s}$ are the sth zeroes of $J'_{\ell+1}(\alpha_{\ell+1,s}) = 0$ and $J_{\ell+1}(\beta_{\ell+1,s}) = 0$, respectively, R_c is the radius of the outer conducting wall, and the prime denotes $(d/dx)J_\ell(x)$. Assuming that the maximum of the function $G_{\ell s'}(x)$ occurs at $x = x_{\ell s'}$, we note that the maximum instability growth rate occurs at a value of R_0/R_c given by $R_0/R_c = x_{\ell s'}/\alpha_{\ell+1,s}$ for the TE mode, and by $R_0/R_c = x_{\ell s'}/\beta_{\ell+1,s}$ for the TM mode. This result is different from that obtained for a hollow electron beam.[8]

A detailed numerical analysis of the TE mode [Eq. (62)] and TM mode [Eq. (63)] dispersion relations is presented in Sec. IV. Two features are noteworthy from the numerical analysis. First, for the optimized value of R_0/R_c, the instability growth rate for the TM mode is comparable to that for the TE mode. Moreover, the growth rate is reduced substantially by introducing a small amount of axial momentum spread ($\Delta/\gamma_b mc \gtrsim 0.01$).

II. EQUILIBRIUM THEORY AND BASIC ASSUMPTIONS

The equilibrium configuration consists of a relativistic electron beam propagating in the combined transverse wiggler and uniform axial guide fields described by

$$\underset{\sim}{B}^0 = -\delta B\cos(\theta - k_0 z)\hat{\underset{\sim}{e}}_r + \delta B\sin(\theta - k_0 z)\hat{\underset{\sim}{e}}_\theta + B_0\hat{\underset{\sim}{e}}_z \ , \tag{1}$$

where B_0 and δB are constants, and k_0 is the axial wavenumber of the helical wiggler field. In Eq. (1), cylindrical polar coordinates (r,θ,z) are used, with z-axis along the propagation direction, and $\hat{\underset{\sim}{e}}_r$, $\hat{\underset{\sim}{e}}_\theta$ and $\hat{\underset{\sim}{e}}_z$ are unit vectors in the r-, θ-, and z-directions, respectively. In the present analysis, we assume that the axial wavenumber of the helical wiggler field is sufficiently large that

$$\frac{\omega_c}{|\omega_0 - \omega_c|}\left|\frac{\delta B}{B_0}\right| \ll k_0 R_0 \ , \tag{2}$$

where $\omega_0 = k_0 V_b$, $\omega_c = eB_0/\gamma_b mc$ is the electron cyclotron frequency, R_0 is the characteristic beam radius, $\gamma_b mc^2$ is the characteristic electron energy, c is the speed of light in <u>vacuo</u>, $V_b = c(\gamma_b^2 - 1)^{1/2}/\gamma_b$ is the mean axial velocity of the electron beam, and -e and m are the electron charge and rest mass, respectively.

It is also assumed that

$$\nu/\gamma_b \ll 1, \tag{3}$$

where $\nu = N_b e^2/mc^2$ is Budker's parameter,

$$N_b = \int_0^{2\pi} d\theta \int_0^{R_c} dr\ r\ n_b^0(r,\ \theta - k_0 z) \ , \tag{4}$$

is the number of electrons per unit axial length of the beam, $n_b^0(r,\ \theta - k_0 z)$ is the equilibrium electron density, and R_c is the radius of the conducting wall. The inequality in Eq. (3) indicates that the beam is very tenuous,

and the perturbed electromagnetic fields, to lowest order, are approximated by the vacuum waveguide fields.[8] Consistent with the low-density assumption in Eq. (3), we also neglect the influence of the (weak) equilibrium self-electric and self-magnetic fields associated with the lack of equilibrium charge and current neutrality.[12]

For present purposes, we assume an equilibrium distribution function of the form[10]

$$f_b^0 = \frac{n_0}{\pi}\,\delta(C_\perp - 2\gamma_b m\omega_b C_h - 2\gamma_b m\hat{T}_\perp)G(C_z)\ , \tag{5}$$

where n_0, ω_b, and $\hat{T}_\perp$ are positive constants, and $C_\perp$, C_h, and C_z are the three single-particle constants of motion defined by[10]

$$C_\perp = p_r^2 + p_\theta^2 + \frac{2eB_0}{ck_0}(p_z - \gamma_b m V_b) - \frac{2e\delta B}{ck_0}\,p_r\cos(\theta - k_0 z) + \frac{2e\delta B}{ck_0}\,p_\theta\sin(\theta - k_0 z)\ , \tag{6}$$

$$C_h = P_\theta + \frac{1}{k_0}(p_z - \gamma_b m V_b) + \frac{e\delta B}{ck_0}\,r\sin(\theta - k_0 z)\ , \tag{7}$$

and

$$\left(C_z - \frac{eB_0}{ck_0}\right)^2 = \left(p_z - \frac{eB_0}{ck_0}\right)^2 + \frac{2e\delta B}{ck_0}\,p_r\cos(\theta - k_0 z) - \frac{2e\delta B}{ck_0}\,p_\theta\sin(\theta - k_0 z)\ . \tag{8}$$

The axial distribution function is normalized according to

$$\int_{-\infty}^{\infty} dC_z\,G(C_z) = 1\ . \tag{9}$$

In Eqs. (6) - (8), $\underset{\sim}{p} = (p_r, p_\theta, p_z) = \gamma m \underset{\sim}{v}$ is the mechanical momentum, $P_\theta = r(p_\theta - eB_0 r/2c)$ is the canonical angular momentum associated with the axial field B_0, and $\gamma mc^2 = (m^2c^4 + c^2\underset{\sim}{p}^2)^{1/2}$ is the relativistic electron energy.

In the parameter regimes of practical interest for free electron laser applications, the axial distribution function $G(C_z)$ is strongly peaked about $C_z = \gamma_b m V_b = \text{const.}$, with characteristic half-width $\Delta C_z \ll \gamma_b m V_b$. Moreover, in the present analysis, it is also assumed that the axial motion is nonresonant with

$$k_0^2 v_z^2 \neq \omega_c^2 , \tag{10}$$

where $v_z = p_z/\gamma m$ is the axial velocity of a typical beam electron. We therefore approximate Eq. (8) by[10]

$$C_z = p_z + \frac{\omega_c \delta B}{(\omega_0 - \omega_c) B_0} [p_r \cos(\theta - k_0 z) - p_\theta \sin(\theta - k_0 z)] . \tag{11}$$

Making use of Eqs. (6), (7), and (11), it is straightforward to show that the combination $C_\perp - 2\gamma_b m \omega_b C_h$ in Eq. (5) can be expressed as[10]

$$\begin{aligned} C_\perp - 2\gamma_b m \omega_b C_h = {} & \left[p_r - \frac{e\delta B}{c k_0} \left(\frac{\omega_0 - \omega_b}{\omega_0 - \omega_c} \right) \cos(\theta - k_0 z) \right]^2 \\ & + \left[p_\theta - \gamma_b m \omega_b r + \frac{e\delta B}{c k_0} \left(\frac{\omega_0 - \omega_b}{\omega_0 - \omega_c} \right) \sin(\theta - k_0 z) \right]^2 \\ & + \gamma_b^2 m^2 \psi_0(r, \theta - k_0 z) , \end{aligned} \tag{12}$$

where $\omega_0 = k_0 V_b$, $\omega_c = eB_0/\gamma_b mc$, and the effective potential $\psi_0(r, \theta - k_0 z)$ is defined by

$$\begin{aligned} \psi_0(r, \theta - k_0 z) = {} & (\omega_b \omega_c - \omega_b^2) r^2 + 2\omega_c \omega_b \left(\frac{\omega_c - \omega_b}{\omega_0 - \omega_c} \right) \frac{r}{k_0} \frac{\delta B}{B_0} \sin(\theta - k_0 z) \\ & - \left(\frac{\omega_0 - \omega_b}{\omega_0 - \omega_c} \right)^2 \frac{\omega_c^2}{\omega_0^2} \left(\frac{\delta B}{B_0} \right)^2 V_b^2 + \frac{2}{\gamma_b m} \left(\frac{\omega_c - \omega_b}{\omega_0} \right) V_b (C_z - \gamma_b m V_b) . \end{aligned} \tag{13}$$

As a simple example, we consider an axial distribution function in which all electrons have a same value of C_z, i.e.,

$$G(C_z) = \delta(C_z - \gamma_b m V_b) \ . \tag{14}$$

After some straightforward algebraic manipulation that makes use of Eqs. (5), (12), and (14), it can readily be shown that the lowest-order (azimuthally symmetric) electron density profile described by Eqs. (5) and (14) can be approximated by[10]

$$n_b^0(r) = \begin{cases} n_0 \ , & 0 \leq r \leq R_0 \ , \\ 0 \ , & R_0 < r < R_c \ , \end{cases} \tag{15}$$

where the mean radius R_0 is defined by

$$R_0^2 = \frac{\left[\frac{2\hat{T}_\perp}{\gamma_b m} + \left(\frac{\omega_0 - \omega_b}{\omega_0 - \omega_c}\right)^2 \frac{\omega_c^2}{\omega_0^2} \left(\frac{\delta B}{B_0}\right)^2 V_b^2\right]}{(\omega_b \omega_c - \omega_b^2)} \ , \tag{16}$$

and use has been made of Eq. (2). Additional general equilibrium properties associated with the distribution function in Eq. (5), including helical distortions of the beam equilibrium for finite $\delta B/B_0$, are discussed in Ref. 10.

III. LINEARIZED VLASOV-MAXWELL EQUATIONS FOR A TENUOUS BEAM

In this section, we make use of the linearized Vlasov-Maxwell equations to investigate the free electron laser stability properties of a relativistic solid electron beam described by the equilibrium distribution function in Eq. (5). We adopt a normal-mode approach in which all perturbations are assumed to vary with time and space according to

$$\delta\psi(\underset{\sim}{x},t) = \sum_{\ell,n} \hat{\psi}_{\ell}^{(n)}(r)\exp\{i[\ell\theta + (k + nk_0)z - \omega t]\} , \tag{17}$$

where $\mathrm{Im}\omega > 0$. Here, ω is the complex eigenfrequency, $k + nk_0$ is the axial wavenumber, and ℓ and n are integers. Moreover, it is also assumed that the perturbations are close to resonance with

$$|\omega - (k + nk_0)V_b| \ll \omega_0, \omega_c , \tag{18}$$

where $\omega_0 = k_0 V_b$ and $\omega_c = eB_0/\gamma_b mc$.

The Maxwell equations for the perturbed electric and magnetic field amplitudes can be expressed as

$$\begin{aligned} \underset{\sim}{\nabla} \times \hat{\underset{\sim}{E}}(\underset{\sim}{x}) &= i(\omega/c)\hat{\underset{\sim}{B}}(\underset{\sim}{x}) , \\ \underset{\sim}{\nabla} \times \hat{\underset{\sim}{B}}(\underset{\sim}{x}) &= (4\pi/c)\hat{\underset{\sim}{J}}(\underset{\sim}{x}) - i(\omega/c)\hat{\underset{\sim}{E}}(\underset{\sim}{x}) , \end{aligned} \tag{19}$$

where

$$\hat{\underset{\sim}{J}}(\underset{\sim}{x}) = -e \int d^3p \, \underset{\sim}{v} \, \hat{f}_b(\underset{\sim}{x},\underset{\sim}{p}) , \tag{20}$$

is the perturbed current density. In Eq. (20),

$$\hat{f}_b(\underset{\sim}{x},\underset{\sim}{p}) = e\int_{-\infty}^{0} d\tau \, \exp(-i\omega t)\left(\hat{\underset{\sim}{E}}(\underset{\sim}{x}') + \frac{\underset{\sim}{v}' \times \hat{\underset{\sim}{B}}(\underset{\sim}{x}')}{c}\right) \cdot \frac{\partial}{\partial \underset{\sim}{p}'} f_b^0 , \tag{21}$$

is the perturbed distribution function, $\tau = t' - t$, and the particle trajectories $\underset{\sim}{x}'(t')$ and $\underset{\sim}{p}'(t')$ satisfy $d\underset{\sim}{x}'/dt' = \underset{\sim}{v}'$ and $d\underset{\sim}{p}'/dt' = -e\underset{\sim}{v}' \times \underset{\sim}{B}^0/c$, with "initial" conditions $\underset{\sim}{x}'(t' = t) = \underset{\sim}{x}$ and $\underset{\sim}{v}'(t' = t) = \underset{\sim}{v}$.

Within the context of Eqs. (3) and (18), the perturbed distribution function in Eq. (21) can be approximated by

$$\hat{f}_b(\underset{\sim}{x},\underset{\sim}{p}) = -\frac{ie}{\omega}\int_{-\infty}^{0} d\tau\, \exp(-i\omega\tau)\Big\{2\Big[\gamma m i\omega(\underset{\sim}{v}' \cdot \hat{\underset{\sim}{E}}) - p_z\Big(\underset{\sim}{v}' \cdot \frac{\partial}{\partial z}\hat{\underset{\sim}{E}}\Big)\Big]\frac{\partial}{\partial p_\perp^2} f_b^0 + \Big(\underset{\sim}{v}' \cdot \frac{\partial}{\partial z}\hat{\underset{\sim}{E}}\Big)\frac{\partial}{\partial p_z} f_b^0\Big\}, \tag{22}$$

where $\gamma = (1 + \underset{\sim}{p}^2/m^2c^2)^{1/2}$, and use has been made of Eq. (19). To lowest order, the axial motion of an electron is free-streaming with[10]

$$z' = z + \frac{p_z}{\gamma m}(t' - t) . \tag{23}$$

Moreover, within the context of Eq. (18), on the right-hand side of Eq. (22) we retain contributions to v_r' and v_θ' in the orbit integral of the form[8]

$$v_r' = v_z \frac{\omega_c}{\omega_0 - \omega_c}\frac{\delta B}{B_0}\cos(\theta - k_0 z - k_0 v_z \tau) , \tag{24}$$

and

$$v_\theta' = -v_z \frac{\omega_c}{\omega_0 - \omega_c}\frac{\delta B}{B_0}\sin(\theta - k_0 z - k_0 v_z \tau) . \tag{25}$$

Finally, since the oscillatory modulation of the radial and azimuthal orbits is small amplitude [Eq. (2)], we approximate

$$r' \simeq r , \quad \theta' \simeq \theta , \tag{26}$$

in the arguments of the perturbation amplitudes on the right-hand side of Eq. (22).

Substituting Eqs. (23) - (26) into Eq. (22), we obtain the perturbed distribution function

$$\hat{f}_b(\underset{\sim}{x},\underset{\sim}{p}) = \sum_{\ell,n} \hat{f}_{b\ell}^{(n)} \exp\{i[\ell\theta + (k + nk_0)z]\}$$

$$= \frac{iec}{\omega} \sum_{\ell,n} \frac{\exp\{i[\ell\theta + (k + nk_0)z]\}}{\omega - (k + nk_0)v_z} \left(\lambda_n \beta_z \hat{E}_{z,\ell}^{(n)}(r) + \frac{e\delta B}{2\gamma mc^2 k_0} \frac{\omega_0}{\omega_0 - \omega_c} \right.$$

$$\left. \times \left\{ \lambda_{n+1} [\hat{E}_{r,\ell-1}^{(n+1)}(r) + i\hat{E}_{\theta,\ell-1}^{(n+1)}(r)] + \lambda_{n-1} [\hat{E}_{r,\ell+1}^{(n-1)}(r) - i\hat{E}_{\theta,\ell+1}^{(n-1)}(r)] \right\} \right), \tag{27}$$

where the function $\lambda_{n'}(\underset{\sim}{p},\omega,k)$ is defined by

$$\lambda_{n'}(\underset{\sim}{p},\omega,k) = 2[\gamma m\omega - (k + n'k_0)p_z] \frac{\partial f_b^0}{\partial p_\perp^2} + (k + n'k_0) \frac{\partial f_b^0}{\partial p_z}, \tag{28}$$

and $\beta_z = v_z/c$. In Eq. (27), the term proportional to λ_n is the longitudinal portion of the perturbed distribution function. Similarly, the terms proportional to λ_{n+1} and λ_{n-1} in Eq. (27) are the transverse electromagnetic portions of the perturbed distribution function.

Consistent with Eq. (18), the eigenfrequency ω can be approximated by $\omega \simeq (k + nk_0)V_b$. We therefore approximate $\omega^2/c^2 - (k + nk_0 + k_0)^2$ by

$$\omega^2/c^2 - (k + nk_0 + k_0)^2 \simeq - \left[\frac{(k + nk_0)^2}{\gamma_b^2} + 2k_0(k + nk_0) + k_0^2 \right] < 0, \tag{29}$$

for $k + nk_0 > 0$. Evidently, Eq. (29) indicates that the n + 1 mode in Eq. (27) is a non-propagating wave in a vacuum waveguide. Without loss of generality, for a tenuous beam, we therefore assume

$$\hat{E}_{r,\ell-1}^{(n+1)}(r) = \hat{E}_{\theta,\ell-1}^{(n+1)}(r) = 0, \tag{30}$$

in the subsequent analysis. Making use of Eq. (30), $\hat{f}_b(\underset{\sim}{x},\underset{\sim}{p})$ in Eq. (27) can then be expressed as

$$\hat{f}_b(\underset{\sim}{x},\underset{\sim}{p}) = \frac{iec}{\omega} \sum_{\ell,n} \frac{\exp\{i[\ell\theta + (k + nk_0)z]\}}{\omega - (k + nk_0)v_z} \left\{\lambda_n \beta_z \hat{E}^{(n)}_{z,\ell}(r) \right.$$

$$\left. + \Lambda\lambda_{n-1}[\hat{E}^{(n-1)}_{r,\ell+1}(r) - i\hat{E}^{(n-1)}_{\theta,\ell+1}(r)]\right\} , \tag{31}$$

where the dimensionless parameter Λ is defined by

$$\Lambda = \frac{e\delta B}{2\gamma_b mc^2 k_0} \frac{\omega_0}{\omega_0 - \omega_c} , \tag{32}$$

and use has been made of the approximation $\gamma \simeq \gamma_b$, which is consistent with Eq. (18).

From Poisson's equation, $\underset{\sim}{\nabla} \cdot \hat{\underset{\sim}{E}}(\underset{\sim}{x}) = 4\pi\hat{\rho}(\underset{\sim}{x})$, and the Maxwell equation (19), we obtain the differential equation,

$$\left[\nabla_\perp^2 + \frac{\omega^2}{c^2} - (k + nk_0)^2\right]\hat{E}^{(n)}_{z,\ell}(r) = \frac{4\pi i(k + nk_0)}{\gamma_b^2} \hat{\rho}^{(n)}_\ell(r) , \tag{33}$$

for the axial (longitudinal) component of the perturbed electric field $\hat{E}^{(n)}_{z,\ell}$. In Eq. (33), $\hat{\rho}^{(n)}_\ell(r) = -e\int d^3p \hat{f}^{(n)}_{b\ell}$ is the perturbed charge density, $\nabla_\perp^2 \equiv r^{-1}(\partial/\partial r)(r\partial/\partial r) - \ell^2/r^2$, and use has been made of $\hat{J}^{(n)}_{z,\ell}(r) \simeq V_b\hat{\rho}^{(n)}_\ell(r)$. In the tenuous beam limit [Eq. (3)], the transverse field components $\hat{\underset{\sim}{E}}^{(n-1)}_{\perp,\ell+1}(r)$ in Eq. (31) can be approximated by the vacuum waveguide fields.[8] In this context, the present stability analysis utilizes the vacuum transverse electric (TE) and transverse magnetic (TM) waveguide modes as a convenient basis to represent the general electromagnetic field perturbation $\hat{\underset{\sim}{E}}^{(n-1)}_{\perp,\ell+1}(r)$, which is determined from[11]

$$\left[\frac{\omega^2}{c^2} - (k + nk_0 - k_0)^2\right]\hat{\underset{\sim}{E}}^{(n-1)}_{\perp,\ell+1}(\underset{\sim}{x})$$

$$= \underset{\sim}{\nabla}_\perp \frac{\partial}{\partial z} \hat{E}^{(n-1)}_{z,\ell+1}(\underset{\sim}{x}) - i\frac{\omega}{c} \hat{\underset{\sim}{e}}_z \times \underset{\sim}{\nabla}_\perp \hat{B}^{(n-1)}_{z,\ell+1}(\underset{\sim}{x}) . \tag{34}$$

Making use of Eqs. (19) and (34), and neglecting the perturbed current density, the vacuum waveguide fields can be expressed as

$$\hat{B}^{(n-1)}_{z,\ell+1}(r) = b_{\ell+1,s} J_{\ell+1}(\alpha_{\ell+1,s} r/R_c) ,$$

$$\hat{E}^{(n-1)}_{r,\ell+1}(r) - i\hat{E}^{(n-1)}_{\theta,\ell+1}(r) = -\frac{\omega R_c}{c\alpha_{\ell+1,s}} b_{\ell+1,s} J_{\ell}(\alpha_{\ell+1,s} r/R_c) , \tag{35}$$

for the TE mode, and

$$\hat{E}^{(n-1)}_{z,\ell+1}(r) = \varepsilon_{\ell+1,s} J_{\ell+1}(\beta_{\ell+1,s} r/R_c) ,$$

$$\hat{E}^{(n-1)}_{r,\ell+1}(r) - i\hat{E}^{(n-1)}_{\theta,\ell+1}(r) = i\frac{(k + nk_0 - k_0)R_c}{\beta_{\ell+1,s}} \varepsilon_{\ell+1,s} J_{\ell}(\beta_{\ell+1,s} r/R_c) , \tag{36}$$

for the TM mode. In Eqs. (35) and (36), $b_{\ell+1,s}$ and $\varepsilon_{\ell+1,s}$ are constants, $J_{\ell'}(x)$ is the Bessel function of first kind of order ℓ', and $\alpha_{\ell+1,s}$ and $\beta_{\ell+1,s}$ are the sth roots of $J'_{\ell+1}(\alpha_{\ell+1,s}) = 0$ and $J_{\ell+1}(\beta_{\ell+1,s}) = 0$, respectively. Here the prime (') denotes $J'_{\ell+1}(x) = (d/dx)J_{\ell+1}(x)$. After some straightforward algebraic manipulation of Eqs. (19), (35), and (36), it can be shown that

$$\left(\frac{\omega^2}{c^2} - (k + nk_0 - k_0)^2 - \frac{\alpha^2_{\ell+1,s}}{R_c^2}\right) b_{\ell+1,s} J_{\ell+1}\left(\frac{\alpha_{\ell+1,s} r}{R_c}\right)$$

$$= -\frac{4\pi}{rc}\left\{\frac{\partial}{\partial r}[r\hat{J}^{(n-1)}_{\theta,\ell+1}(r)] - i(\ell + 1)\hat{J}^{(n-1)}_{r,\ell+1}(r)\right\} , \tag{37}$$

for the TE mode, and

$$\left(\frac{\omega^2}{c^2} - (k + nk_0 - k_0)^2 - \frac{\beta^2_{\ell+1,s}}{R_c^2}\right) \varepsilon_{\ell+1,s} J_{\ell+1}\left(\frac{\beta_{\ell+1,s} r}{R_c}\right)$$

$$= 4\pi i\left[(k + nk_0 - k_0)\hat{\rho}^{(n-1)}_{\ell+1}(r) - \frac{\omega}{c^2}\hat{J}^{(n-1)}_{z,\ell+1}(r)\right] , \tag{38}$$

for the TM mode. Moreover, making use of the continuity equation,

$$i\omega\hat{\rho}^{(n-1)}_{\ell+1} - i(k + nk_0 - k_0)\hat{J}^{(n-1)}_{z,\ell+1} = \frac{1}{r}\frac{\partial}{\partial r}[r\hat{J}^{(n-1)}_{r,\ell+1}] + \frac{i(\ell + 1)}{r}\hat{J}^{(n-1)}_{\theta,\ell+1} , \tag{39}$$

the approximation $\hat{J}^{(n-1)}_{z,\ell+1}(r) \simeq V_b \hat{\rho}^{(n-1)}_{\ell+1}(r)$ [consistent with Eq. (3)], and approximating $k + nk_0 \simeq k_0/(1 - V_b/c)$ on the right-hand side of Eq. (38), we find that Eq. (38) can be expressed as

$$\left\{\frac{\omega^2}{c^2} - (k + nk_0 - k_0)^2 - \frac{\beta^2_{\ell+1,s}}{R_c^2}\right\} \varepsilon_{\ell+1,s} J_{\ell+1}\left(\frac{\beta_{\ell+1,s} r}{R_c}\right)$$

$$= \frac{4\pi}{rc}\left\{\frac{\partial}{\partial r}\left[r\hat{J}^{(n-1)}_{r,\ell+1}(r)\right] + i(\ell+1)\hat{J}^{(n-1)}_{\theta,\ell+1}(r)\right\} , \tag{40}$$

for the TM mode.

For convenience of notation in the subsequent analysis, we introduce the effective susceptibility,

$$\chi_{n,n'}(\omega,k) = 4\pi e^2 \int d^3p \, \frac{\lambda_{n'}(p,\omega,k)}{\omega - (k + nk_0)v_z} . \tag{41}$$

Moreover, to simplify the present analysis, we also assume that the beam rotation is slow with

$$\omega_b << \omega_c, \omega_0 . \tag{42}$$

Within the context of Eq. (42), we can show from Eq. (12) that the equilibrium distribution function is an even function of

$$p_r - 2\gamma_b mc\Lambda\cos(\theta - k_0 z) \tag{43}$$

and

$$p_\theta + 2\gamma_b mc\Lambda\sin(\theta - k_0 z) , \tag{44}$$

for the beam rotations satisfying $\omega_b << \omega_c, \omega_0$. Making use of Eqs. (31), (41), and (43), the perturbed charge and current densities are given by

$$\hat{J}^{(n-1)}_{\theta,\ell+1}(r) = \frac{c^2\Lambda}{4\pi\omega} G_\ell(\omega,k,r) = i\hat{J}^{(n-1)}_{r,\ell+1}(r) = ic\Lambda\hat{\rho}^{(n)}_\ell(r) , \tag{45}$$

where the function $G_\ell(\omega,k,r)$ is defined by

$$G_{\ell}(\omega,k,r) = \chi_{n,n}\beta_z \hat{E}^{(n)}_{z,\ell}(r)$$

$$+ \Lambda\chi_{n,n-1}[\hat{E}^{(n-1)}_{r,\ell+1}(r) - i\hat{E}^{(n-1)}_{\theta,\ell+1}(r)] \; . \tag{46}$$

Equations (33), (37), and (40), when combined with Eq. (45), constitute one of the principal results of this paper and can be used to investigate stability properties for a broad range of system parameters. Moreover, in limiting cases, the dispersion relation for the free electron laser instability can be obtained in a closed form (Sec. IV).

IV. FREE ELECTRON LASER STABILITY PROPERTIES

In this section, simplified expressions are obtained for the longitudinal perturbations in Eq. (33), and the results are used to derive the dispersion relation for several values of azimuthal harmonic number ℓ. The present analysis assumes short wavelength perturbations with

$$|q_n^2| = |(k + nk_0)^2 - \omega^2/c^2| >> 1/R_0^2 . \tag{47}$$

Moreover, for $\omega \simeq (k + nk_0)V_b$ and $k + nk_0 \simeq k_0/(1 - V_b/c)$, the inequality in Eq. (47) can be expressed in the equivalent form,

$$(1 + V_b/c)^2\gamma_b^2 k_0^2 R_0^2 >> 1 , \tag{48}$$

which is readily satisfied in the parameter regimes of present experimental interest. As shown in Appendix A, for short wavelength perturbations satisfying Eq. (48), the axial component of the perturbed electric field $\hat{E}_{z,\ell}^{(n)}(r)$ in Eq. (33) can be approximated by

$$\hat{E}_{z,\ell}^{(n)}(r) = \begin{cases} \hat{\phi}_{\ell,s'} J_\ell(\beta_{\ell,s'} r/R_0) , & 0 \leq r < R_0 , \\ 0 , & \text{otherwise} . \end{cases} \tag{49}$$

In Eq. (49), $\beta_{\ell,s'}$ is the s'th root of $J_\ell(\beta_{\ell,s'}) = 0$, and $\hat{\phi}_{\ell,s'}$ is a constant.

Substituting Eqs. (35) and (49) into Eq. (46), multiplying Eqs. (33) and (37) by $rJ_\ell(\beta_{\ell,s'} r/R_0)$ and $rJ_{\ell+1}(\alpha_{\ell+1,s} r/R_c)$, respectively, and integrating from $r = 0$ to $r = R_c$, we obtain two homogeneous equations relating the perturbation amplitudes $\hat{\phi}_{\ell,s'}$ and $b_{\ell+1,s}$. For the TE mode polarization, these are

$$\hat{\phi}_{\ell,s'} \int_0^{R_c} dr\, r\, \Theta(R_0 - r) \left(\frac{1}{\gamma_b^2} \chi_{n,n} + q_n^2 + \frac{\beta_{\ell,s'}^2}{R_0^2} \right) J_\ell^2 \left(\frac{\beta_{\ell,s'} r}{R_0} \right) \tag{50}$$

$$= \frac{(k + nk_0)R_c}{\gamma_b^2 \alpha_{\ell+1,s}} \Lambda b_{\ell+1,s} \int_0^{R_c} dr\, r\, \chi_{n,n-1} J_\ell\left(\frac{\alpha_{\ell+1,s} r}{R_c}\right) J_\ell\left(\frac{\beta_{\ell,s'} r}{R_0}\right),$$

and

$$b_{\ell+1,s} \int_0^{R_c} dr\, r \left[\frac{\omega^2}{c^2} - (k + nk_0 - k_0)^2 - \frac{\alpha_{\ell+1,s}^2}{R_c^2} + \Lambda^2 \chi_{n,n-1}\right] J_{\ell+1}^2\left(\frac{\alpha_{\ell+1,s} r}{R_c}\right) \tag{51}$$

$$= \frac{\beta_{\ell,s'}}{(k + nk_0)R_0} \Lambda \hat{\phi}_{\ell,s'} \int_0^{R_c} dr\, r \Theta(R_0 - r) \chi_{n,n} J_\ell\left(\frac{\beta_{\ell,s'} r}{R_0}\right) J_{\ell+1}\left(\frac{\alpha_{\ell+1,s} r}{R_c}\right),$$

where $\Theta(x)$ is the Heaviside step function defined by

$$\Theta(x) = \begin{cases} 1, & x > 0, \\ 0, & \text{otherwise}. \end{cases} \tag{52}$$

Similarly, for the TM mode polarization, we obtain

$$\hat{\phi}_{\ell,s'} \int_0^{R_c} dr\, r\, \Theta(R_0 - r) \left(\frac{1}{\gamma_b^2} \chi_{n,n} + q_n^2 + \frac{\beta_{\ell,s'}^2}{R_0^2}\right) J_\ell^2\left(\frac{\beta_{\ell,s'} r}{R_0}\right)$$

$$= -i \frac{(k + nk_0)R_c}{\gamma_b^2 \beta_{\ell+1,s}} \Lambda \varepsilon_{\ell+1,s} \int_0^{R_c} dr\, r\, \chi_{n,n-1} J_\ell\left(\frac{\beta_{\ell+1,s} r}{R_c}\right) J_\ell\left(\frac{\beta_{\ell,s'} r}{R_0}\right), \tag{53}$$

and

$$\varepsilon_{\ell+1,s} \int_0^{R_c} dr\, r \left[\frac{\omega^2}{c^2} - (k + nk_0 - k_0)^2 - \frac{\beta_{\ell+1,s}^2}{R_c^2} + \Lambda^2 \chi_{n,n-1}\right] J_{\ell+1}^2\left(\frac{\beta_{\ell+1,s} r}{R_c}\right)$$

$$= i \frac{\beta_{\ell,s'}}{(k + nk_0)R_0} \Lambda \hat{\phi}_{\ell,s'} \int_0^{R_c} dr\, r\, \Theta(R_0 - r) \chi_{n,n} J_{\ell+1}\left(\frac{\beta_{\ell,s'} r}{R_0}\right) \tag{54}$$

$$\times J_{\ell+1}\left(\frac{\beta_{\ell+1,s} r}{R_c}\right),$$

where use has been made of $\omega \simeq (k + nk_0)V_b$ and $(k + nk_0) \simeq k_0/(1 - V_b/c)$.

In the present analysis, it is assumed that the axial distribution function has the form

$$G(C_z) = \frac{\Delta}{\pi} \frac{1}{(C_z - \gamma_b m V_b)^2 + \Delta^2}, \tag{55}$$

where Δ is the characteristic spread in C_z about the mean value $C_z = \gamma_b m V_b$.

We further assume that the characteristic spread Δ is small in comparison with $\gamma_b m V_b$. Substituting Eqs. (5) and (55) into Eqs. (28) and (41), we obtain the approximate expression

$$\chi_{n,n'} = \begin{cases} \dfrac{4\nu}{\gamma_b R_0^2} \dfrac{\omega^2 - (k + nk_0)(k + n'k_0)c^2}{[\omega - (k + nk_0)V_b + i|k + nk_0|\Delta/\gamma_b^3 m]^2}, & 0 \le r < R_0, \\ 0, & R_0 < r \le R_c \end{cases} \tag{56}$$

In obtaining Eq. (56), use has been made of Eq. (18). Making use of the definition of Budker's parameter in Eqs. (3) and (4), the term $4\nu/\gamma_b R_0^2$ in Eq. (56) can also be expressed as $4\nu/\gamma_b R_0^2 = \omega_{pb}^2/c^2$, where $\omega_{pb}^2 = 4\pi n_0 e^2/\gamma_b m$ is the plasma frequency-squared.

The condition for a nontrivial solution to Eqs. (50) and (51) is that the determinant of the coefficients $\hat{\phi}_{\ell,s'}$ and $b_{\ell+1,s}$ be equal to zero. After some algebraic manipulation, we find that the TE mode dispersion relation can be expressed as

$$\left(\omega - (k + nk_0)V_b + i\frac{|k + nk_0|\Delta}{\gamma_b^3 m}\right)^2 \left\{\frac{\omega^2}{c^2} - (k + nk_0 - k_0)^2 - \frac{\alpha_{\ell+1,s}^2}{R_c^2}\right\}$$

$$\times \left\{\left[\omega - (k + nk_0)V_b + i\frac{|k + nk_0|\Delta}{\gamma_b^3 m}\right]^2 - 4\frac{\nu c^2}{\gamma_b^3 R_0^2}\right\}$$

$$= 4\Lambda^2 \frac{\nu c^2}{\gamma_b R_c^2}\left[k_0(k + nk_0 - k_0) - \frac{\alpha_{\ell+1,s}^2}{R_c^2}\right] Q^E_{\ell ss'}\left(\frac{\alpha_{\ell+1,s}R_0}{R_c}\right)\left\{4\frac{\nu c^2}{\gamma_b^3 R_0^2}\right.$$

$$\left. + H_{\ell ss'}\left(\frac{\alpha_{\ell+1,s}R_0}{R_c}\right)\left[\omega - (k + nk_0)V_b + i\frac{|k + nk_0|\Delta}{\gamma_b^3 m}\right]^2\right.$$

$$\left. - 4\frac{\nu c^2}{\gamma_b^3 R_0^2} H_{\ell ss'}\left(\frac{\alpha_{\ell+1,s}R_0}{R_c}\right)\right\}, \tag{57}$$

where the coupling coefficient $Q^E_{\ell ss'}(\alpha_{\ell+1,s}R_0/R_c)$ is defined by

$$Q^E_{\ell ss'}(x) = \frac{\alpha_{\ell+1,s}^2}{\alpha_{\ell+1,s}^2 - (\ell + 1)^2} \frac{G_{\ell s'}(x)}{J_{\ell+1}^2(\alpha_{\ell+1,s})}, \tag{58}$$

and the functions $G_{\ell s'}(x)$ and $H_{\ell ss'}(x)$ are defined by

$$G_{\ell s'}(x) = 4\beta^2_{\ell,s'} \frac{J^2_\ell(x)}{(x^2 - \beta^2_{\ell,s'})^2} \tag{59}$$

and

$$H_{\ell ss'}(x) = \frac{J^2_{\ell+1}(x) - J_\ell(x)J_{\ell+2}(x)}{G_{\ell s'}(x)} \ . \tag{60}$$

In Eq. (57), the subscript s and s' represent the radial mode numbers of the transverse and longitudinal perturbations, respectively.

For small wiggler amplitude ($\Lambda \ll 1$), we investigate free electron laser stability properties for ω and $k + nk_0$ near the simultaneous zeros of the transverse dispersion relation, $\omega^2 - (k + nk_0 - k_0)^2c^2 - \alpha^2_{\ell+1,s}c^2/R_c^2 = 0$, and the longitudinal dispersion relation

$$\left(\omega - (k + nk_0)V_b + i \frac{|k + nk_0|\Delta}{\gamma_b^3 m}\right)^2 - 4 \frac{\nu c^2}{\gamma_b^3 R_0^2} = 0 \ . \tag{61}$$

In this regard, making use of Eq. (61), the TE mode dispersion relation in Eq. (57) can be approximated by

$$\left\{\frac{\omega^2}{c^2} - (k + nk_0 - k_0)^2 - \frac{\alpha^2_{\ell+1,s}}{R_c^2}\right\}\left\{\left(\omega - (k + nk_0)V_b + i \frac{|k + nk_0|\Delta}{\gamma_b^3 m}\right)^2 - 4 \frac{\nu c^2}{\gamma_b^3 R_0^2}\right\} = 4\Lambda^2 \frac{\nu c^2}{\gamma_b R_c^2}\left[k_0(k + nk_0 - k_0) - \frac{\alpha^2_{\ell+1,s}}{R_c^2}\right] Q^E_{\ell ss'}\left(\frac{\alpha_{\ell+1,s}R_0}{R_c}\right). \tag{62}$$

In a similar manner, from Eqs. (53) and (54), we obtain the approximate TM mode dispersion relation,

$$\left\{\frac{\omega^2}{c^2} - (k + nk_0 - k_0)^2 - \frac{\beta^2_{\ell+1,s}}{R_c^2}\right\}\left\{\left(\omega - (k + nk_0)V_b + i \frac{|k + nk_0|\Delta}{\gamma_b^3 m}\right)^2 - 4 \frac{\nu c^2}{\gamma_b^3 R_0^2}\right\} = 4\Lambda^2 \frac{\nu c^2}{\gamma_b R_c^2}\left[k_0(k + nk_0 - k_0) - \frac{\beta^2_{\ell+1,s}}{R_c^2}\right] Q^M_{\ell ss'}\left(\frac{\beta_{\ell+1,s}R_0}{R_c}\right), \tag{63}$$

where the TM mode coupling coefficient $Q^M_{\ell ss'}(\beta_{\ell+1,s}R_0/R_c)$ is defined by

$$Q^M_{\ell ss'}(x) = G_{\ell s'}(x)/J^2_{\ell+2}(\beta_{\ell+1,s}) \ , \tag{64}$$

and the function $G_{\ell s'}(x)$ is defined in Eq. (59).

Figure 1 shows plots of $G_{\ell s'}(x)$ versus x obtained from Eq. (59) for (a) $\beta_{\ell,s'} = \beta_{0,1}$ and (b) $\beta_{\ell,s'} = \beta_{1,3}$. Except in the case $\beta_{\ell,s'} = \beta_{0,1}$, the plots of $G_{\ell,s'}(x)$ for arbitrary $\beta_{\ell,s'}$ are similar to those for $\beta_{\ell,s'} = \beta_{1,3}$ in Fig. 1(b). As shown in Fig. 1(b), the quantities $G^{\phi}_{\ell s'} \equiv G_{\ell s'}(x_{\ell s'})$ and $x_{\ell s'}$ denote the maximum value of $G_{\ell s'}(x)$ and the corresponding value of x for a specified $\beta_{\ell,s'}$. For example, in Fig. 1, $(x_{\ell s'}, G^{\phi}_{\ell s'}) = (0, 0.69)$ for $\beta_{\ell,s'} = \beta_{0,1}$ and $(x_{\ell s'}, G^{\phi}_{\ell s'}) = (9.8, 0.064)$ for $\beta_{\ell,s'} = \beta_{1,3}$. Shown in Fig. 2 are plots of (a) $x_{\ell s'}$ and (b) the corresponding values of $G^{\phi}_{\ell s'} = G_{\ell s'}(x_{\ell s'})$ for several different values of the azimuthal and radial mode numbers ℓ and s'. It is evident from Fig. 2(b) that $G^{\phi}_{\ell s'}$ decreases rapidly with increasing values of the mode numbers ℓ and s'. Moreover, we note from Fig. 2(a) that $x_{\ell s'}$ can be approximated by

$$x_{\ell s'} \simeq \beta_{\ell,s'}, \quad s' \neq 1 . \tag{65}$$

In this regard, for $s' \neq 1$, $G^{\phi}_{\ell s'}$ can be approximated by

$$G^{\phi}_{\ell s'} \simeq G_{\ell s'}(\beta_{\ell,s'}) = J^2_{\ell+1}(\beta_{\ell,s'}), \; s' \neq 1. \tag{66}$$

Shown in Fig. 3 are plots of (a) $Q^{E}_{\ell ss'}/G_{\ell s'}$ for the TE mode and (b) $Q^{M}_{\ell ss'}/G_{\ell s'}$ for the TM mode, obtained from Eqs. (58) and (64) respectively. Note that the curves in Fig. 3 are independent of the longitudinal radial mode number s'. Evidently, the values of $Q^{E}_{\ell ss'}/G_{\ell s'}$ and $Q^{M}_{\ell ss'}/G_{\ell s'}$ increase with increasing values of azimuthal and transverse radial mode numbers, ℓ and s. After careful examination of Eqs. (58) and (64), we find that the maximum coupling between the transverse and longitudinal modes occurs for a value of R_0/R_c given by

$$R_0/R_c = \begin{cases} x_{\ell s'}/\alpha_{\ell+1,s} , & \text{TE mode} , \\ x_{\ell s'}/\beta_{\ell+1,s} , & \text{TM mode} . \end{cases} \tag{67}$$

Equation (67) is valid only when $x_{\ell s'} \leq \alpha_{\ell+1,s}$ for the TE mode, and $x_{\ell s'} \leq \beta_{\ell+1,s}$ for the TM mode. For $x_{\ell s'} > \alpha_{\ell+1,s}$ (TE), or $x_{\ell s'} > \beta_{\ell+1,s}$ (TM), the maximum coupling occurs for $R_0/R_c = 1$. The maximum coupling coefficients corresponding to Eq. (67) can be determined from Figs. 2(b) and 3. For example, for $(\ell,s,s') = (3,2,1)$, we determine that the maximum coupling coefficient and the corresponding ratio R_0/R_c, are given by $(Q^E_{\ell ss'}, R_0/R_c) = (1.607, 0.625)$ for the TE mode, and $(Q^M_{\ell ss'}, R_0/R_c)$ $(1.83, 0.52)$ for the TM mode.

It is instructive to examine the present results for perturbations with the lowest mode numbers, i.e., $(\ell,s,s') = (0,1,1)$, particularly for a beam-filled waveguide with $R_0/R_c = 1$. In this limit, from Fig. 1(a), we obtain $G_{\ell s'}(\alpha_{1,1}) = 0.4$ for the TE mode, and $G_{\ell s'}(\beta_{1,1}) = 0.045$ mode. We therefore conclude that the TE mode polarization is the most unstable. Multiplying $G_{\ell s'}(\alpha_{1,1}) = 0.4$ by $Q^E_{\ell ss'}/G_{\ell s'} = 4.2$ in Fig. 3(a), the coupling coefficient is given by $Q^E_{011} = 1.7$. Assuming zero axial momentum spread ($\Delta = 0$) and short axial wavelengths ($k_0^2 R_c^2 >> 1$), the TE mode dispersion relation in Eq. (62) can be approximated by

$$\left(\frac{\omega^2}{c^2} - (k + nk_0 - k_0)^2 \right) \left\{ [\omega - (k + nk_0)V_b]^2 - \frac{\omega_{pb}^2}{\gamma_b^2} \right\} = 3.4 \Lambda^2 \omega_{pb}^2 k_0^2 , \tag{68}$$

for the $(\ell,s,s') = (0,1,1)$ perturbation and $R_0/R_c = 1$. Equation (68) is similar in form to the result obtained by Davidson and Uhm[3] for a uniform density beam with infinite cross section. In particular, the constant numerical factor on the right-hand side of Eq. (68) is equal to 3.4, whereas in Ref. 3 the constant numerical factor is equal to 8.

Finally, we have investigated detailed stability properties by solving the dispersion relations in Eqs. (62) and (63) numerically for a broad range of system parameters. Defining the normalized Doppler-shifted eigenfrequency by

$$\Omega = [\omega - (k + nk_0)V_b]/k_0c \ , \tag{69}$$

we calculate the normalized growth rate $\Omega_i = \mathrm{Im}\Omega$ from Eqs. (62) and (63). Shown in Fig. 4 are plots of the normalized growth rate Ω_i versus $(k + nk_0)/k_0$ for $(\ell,s,s') = (3,2,1)$, $k_0R_c = 10$, $\gamma_b = 10$, $\nu/\gamma_b = 0.02$, and $\Lambda^2 = 0.01$, with (a) $R_0/R_c = x_{31}/\alpha_{4,2}$ for the TE mode, and (b) $R_0/R_c = x_{31}/\beta_{4,2}$ for the TM mode. For these optimized choices of R_0/R_c, the instability growth rate for the TM mode is comparable to that for the TE mode. Moreover, the growth rate is reduced substantially by introducing a small amount of axial momentum spread ($\Delta/\gamma_b mc \lesssim 0.01$).

We conclude this section by pointing out two areas in which the analysis can be extended. First, the restriction to very short wavelength perturbations [Eq. (48)] can be removed in a relatively straightforward manner. Second, paralleling the self-consistent theoretical formalism developed in previous studies,[8] the stability analysis can also be carried out without making the approximation that the transverse perturbations are represented by the vacuum waveguide fields.

V. CONCLUSIONS

In this paper, we have examined the free electron laser instability for a solid relativistic electron beam propagating in the combined transverse wiggler and uniform axial guide field given in Eq. (1). The analysis was carried out within the framework of the linearized Vlasov-Maxwell equations. The equilibrium (Sec. II) and stability (Secs. III and IV) properties were investigated in detail for the choice of distribution function in which all electrons have the same value of the linear combination of transverse and helical invariants, $C_\perp - 2\gamma_b m\omega_b C_h$, and a Lorentzian distribution in the axial invariant C_z [Eqs. (5) and (18)]. One of the most important conclusions of this analysis is that the maximum instability growth rate for a solid electron beam is comparable to that of a hollow beam with similar parameters.[8] Moreover, it is also found that the maximum growth rate occurs at a value of R_0/R_c corresponding to $R_0/R_c = x_{\ell s}'/\alpha_{\ell+1,s}$ for TE mode perturbations, and $R_0/R_c = x_{\ell s}'/\beta_{\ell+1,s}$ for TM mode perturbations. For these optimized values of R_0/R_c, the instability growth rate for the TM mode is comparable to that for the TE mode. Moreover, the growth rate is substantially reduced by introducing a small amount of axial momentum spread ($\Delta/\gamma_b mc \gtrsim 0.01$).

ACKNOWLEDGMENTS

This research was supported in part by Defense Advance Research Project Agency (DOD) under ARPA Order No. 3718, Amendment No. 12, in part by the Independent Research Fund at the Naval Surface Weapons Center, and in part by the Office of Naval Research.

REFERENCES

1. T. C. Marshall, S. Talmadge, and P. Efthimion, Appl. Phys. Lett. 31, 320 (1977).
2. D. A. G. Deacon, L. R. Elias, J. M. M. Madey, G. J. Ramian, H. A. Schwettman, and T. I. Smith, Phys. Rev. Lett. 38, 897 (1977).
3. R. C. Davidson and H. S. Uhm, Phys. Fluids 23, 2076 (1980).
4. A. T. Lin and J. M. Dawson, Phys. Fluids 23, 1224 (1980).
5. P. Sprangle, C. M. Tang, and W. M. Manheimer, Phys. Rev. A21, 302 (1980).
6. I. B. Bernstein and J. L. Hirshfield, Phys. Rev. A20, 1661 (1979).
7. H. S. Uhm and R. C. Davidson, "Theory of Free Electron Laser Instability in a Relativistic Annular Electron Beam", submitted for publication (1980).
8. H. S. Uhm and R. C. Davidson, "Free Electron Laser Instability for a Relativistic Annular Electron Beam in a Helical Wiggler Field", submitted for publication (1980).
9. J. R. Bayless, Bull. Am. Phys. Soc. 25, 753 (1980).
10. R. C. Davidson and H. S. Uhm, "Helically Distorted Relativistic Electron Beam Equilibria for Free Electron Laser Applications", submitted for publication (1980).
11. J. D. Jackson, Classical Electrodynamics (John Wiley & Sons, Inc., New York, 1962), Ch. 8.
12. R. C. Davidson, Theory of Nonneutral Plasmas (Benjamin, Reading, Mass., 1974), Ch. 2.

FIGURE CAPTIONS

Fig. 1 Plots of $G_{\ell s'}(x)$ versus x [Eq. (59)] for (a) $\beta_{\ell,s'} = \beta_{0,1}$ and (b) $\beta_{\ell,s'} = \beta_{1,3}$.

Fig. 2 Plots of (a) $x_{\ell s'}$ and (b) the corresponding $G^{\phi}_{\ell s'} = G_{\ell s'}(x_{\ell s'})$ for several values of azimuthal and radial mode numbers, ℓ and s'.

Fig. 3 Plots of (a) $Q^{E}_{\ell ss'}/G_{\ell s'}$ and (b) $Q^{M}_{\ell ss'}/G_{\ell s'}$ [Eqs. (58) and (64)] for several values of ℓ and s.

Fig. 4 Plots of normalized growth rate Ω_i versus $(k + nk_0)/k_0$ for $(\ell,s,s') = (3,2,1)$, $\gamma_b = 10$, $\nu/\gamma_b = 0.02$, and $\Lambda^2 = 0.01$, with (a) $R_0/R_c = x_{31}/\alpha_{4,2}$ for the TE mode and (b) $R_0/R_c = x_{31}/\beta_{4,2}$ for the TM mode.

APPENDIX A

LONGITUDINAL PERTURBATIONS FOR THE FREE ELECTRON LASER INSTABILITY

In this Appendix, we investigate properties of the longitudinal perturbations about an electron beam propagating through a cylindrical waveguide with radius R_c. In the present analysis, it is assumed that the perturbations have short wavelength with

$$|q_n^2| = |(k + nk_0)^2 - \omega^2/c^2| >> 1/R_0^2 , \tag{A.1}$$

which can also be expressed as

$$q_n^2 R_0^2 \simeq (1 + V_b/c)^2 \gamma_b^2 k_0^2 R_0^2 >> 1 , \tag{A.2}$$

for the frequencies of interest for free electron laser applications. Equation (A.2) is easily satisfied in parameter regimes of present experimental interest. In the limit of a small wiggler amplitude ($\Lambda \to 0$), we obtain the longitudinal eigenvalue equation,

$$\left(\frac{1}{r} \frac{\partial}{\partial r} r \frac{\partial}{\partial r} - \frac{\ell^2}{r^2} - q_n^2 \right) \hat{E}_{z,\ell}^{(n)}(r) = - \frac{(\omega_{pb}^2/\gamma_b^2) q_n^2 \hat{E}_{z,\ell}^{(n)}(r) \Theta(R_0 - r)}{[\omega - (k + nk_0)V_b + i|k + nk_0|\Delta/\gamma_b^3 m]^2} , \tag{A.3}$$

from Eqs. (33), (45), (46), and (56). In Eq. (A.3), $\Theta(x)$ is the Heaviside step function defined in Eq. (52), and $\omega_{pb}^2 = 4\nu c^2/\gamma_b R_0^2$ is the plasma-frequency-squared.

For notational simplicity, we define

$$\delta\phi^{\ell}(r) \equiv \hat{E}_{z,\ell}^{(n)}(r) . \tag{A.4}$$

Inside the electron beam ($0 \leq r < R_0$), Eq. (A.3) can be expressed as[12]

$$\left(\frac{1}{r}\frac{\partial}{\partial r}\, r\, \frac{\partial}{\partial r} - \frac{\ell^2}{r^2} + T^2\right)\delta\phi^{\ell}(r) = 0 \ , \quad 0 \le r < R_0 \ , \tag{A.5}$$

where

$$T^2 \equiv q_n^2 \left\{ \frac{\omega_{pb}^2/\gamma_b^2}{[\omega - (k + nk_0)V_b + i|k + nk_0|\Delta/\gamma_b^3 m]^2} - 1 \right\} . \tag{A.6}$$

Outside the electron beam ($R_0 < r < R_c$), Eq. (A.3) reduces to the free-space eigenvalue equation

$$(\frac{1}{r}\frac{\partial}{\partial r}\, r\, \frac{\partial}{\partial r} - \frac{\ell^2}{r^2} - q_n^2)\delta\phi^{\ell}(r) = 0 \ , \quad R_0 < r < R_c \ . \tag{A.7}$$

The solution to Eq. (A.5) that remains finite at r = 0 is

$$\delta\phi_{in}^{\ell}(r) = \hat{\phi}_{\ell} J_{\ell}(TR) \ , \quad 0 \le r < R_0 \ , \tag{A.8}$$

where $J_{\ell}(x)$ is the Bessel function of the first kind of order ℓ, and $\hat{\phi}_{\ell}$ is a constant. Noting $q_n^2 R_0^2 >> 1$ in Eq. (A.2), we can express the solution to Eq. (A.7) as

$$\delta\phi_{out}^{\ell}(r) = C[I_{\ell}(q_n r)K_{\ell}(q_n R_c) - K_{\ell}(q_n r)I_{\ell}(q_n R_c)], \quad R_0 < r \le R_c, \tag{A.9}$$

where I_{ℓ} and K_{ℓ} are modified Bessel functions of order ℓ, and C is a constant.

The boundary conditions on $\delta\phi^{\ell}(r)$ at the surface of the electron beam are given by

$$[\delta\phi_{in}^{\ell}]_{r=R_0} = [\delta\phi_{out}^{\ell}]_{r=R_0} \ , \tag{A.10}$$

and

$$[(\partial/\partial r)\delta\phi_{in}^{\ell}]_{r=R_0} = [(\partial/\partial r)\delta\phi_{out}^{\ell}]_{r=R_0} \ , \tag{A.11}$$

from Eq. (A.3). Substituting Eqs. (A.8) and (A.9) into Eqs. (A.10) and (A.11) gives

$$TR_0 \frac{J'_\ell(TR_0)}{J_\ell(TR_0)} = h(q_n)$$

$$\equiv q_n R_0 \frac{I'_\ell(q_n R_0)K_\ell(q_n R_c) - I_\ell(q_n R_c)K'_\ell(q_n R_0)}{I_\ell(q_n R_0)K_\ell(q_n R_c) - I_\ell(q_n R_c)K_\ell(q_n R_0)} , \tag{A.12}$$

where the "prime" notation denotes derivative with respect to the complete argument of the Bessel function, e.g., $J'_\ell(TR_0) = [dJ_\ell(x)/dx]_{x=TR_0}$. The expression for the longitudinal wave admittance $h(q_n)$ in Eq. (A.12) can be simplified in several limiting cases, including short wavelength perturbations with $|q_n^2 R_0^2| >> 1$. In this case, $h(q_n)$ can be approximated by

$$h(q_n) = -q_n R_0 \coth q_n(R_c - R_0) , \tag{A.13}$$

and Eq. (A.12) reduces to

$$-TR_0 \frac{J'_\ell(TR_0)}{J_\ell(TR_0)} = q_n R_0 \coth q_n(R_c - R_0) . \tag{A.14}$$

Evidently, the right-hand side of Eq.(A.14)is a very large positive number, and the lowest-order longitudinal dispersion relation (for $\Lambda \to 0$) can be approximated by

$$J_\ell(TR_0) \simeq 0 , \tag{A.15}$$

where T is defined in Eq. (A.6). It follows from Eq. (A.15) that

$$T^2 R_0^2 = \beta^2_{\ell,s'} , \quad s' = 1, 2, \ldots , \tag{A.16}$$

where $\beta_{\ell,s'}$ is the s'th zero of $J_\ell(x) = 0$. In this regard, Eqs. (A.8) and (A.9) can be approximated by

$$\delta\phi^\ell(r) = \begin{cases} \hat{\phi}_{\ell,s'} J_\ell(\beta_{\ell,s'} r/R_0) , & 0 \leq r < R_0 , \\ 0 , & \text{otherwise} , \end{cases} \tag{A.17}$$

where $\hat{\phi}_{\ell,s'}$ is a constant. Substituting Eq. (A.6) into Eq. (A.16)

and making use of Eq. (A.2), we obtain the longitudinal dispersion relation,

$$\left[\omega - (k + nk_0)V_b + i\frac{|k + nk_0|\Delta}{\gamma_b^3 m}\right]^2 - \frac{\omega_{pb}^2}{\gamma_b^2} = 0 \ , \qquad (A.18)$$

where the term proportional to $\beta_{\ell,s}^2$, has been neglected.

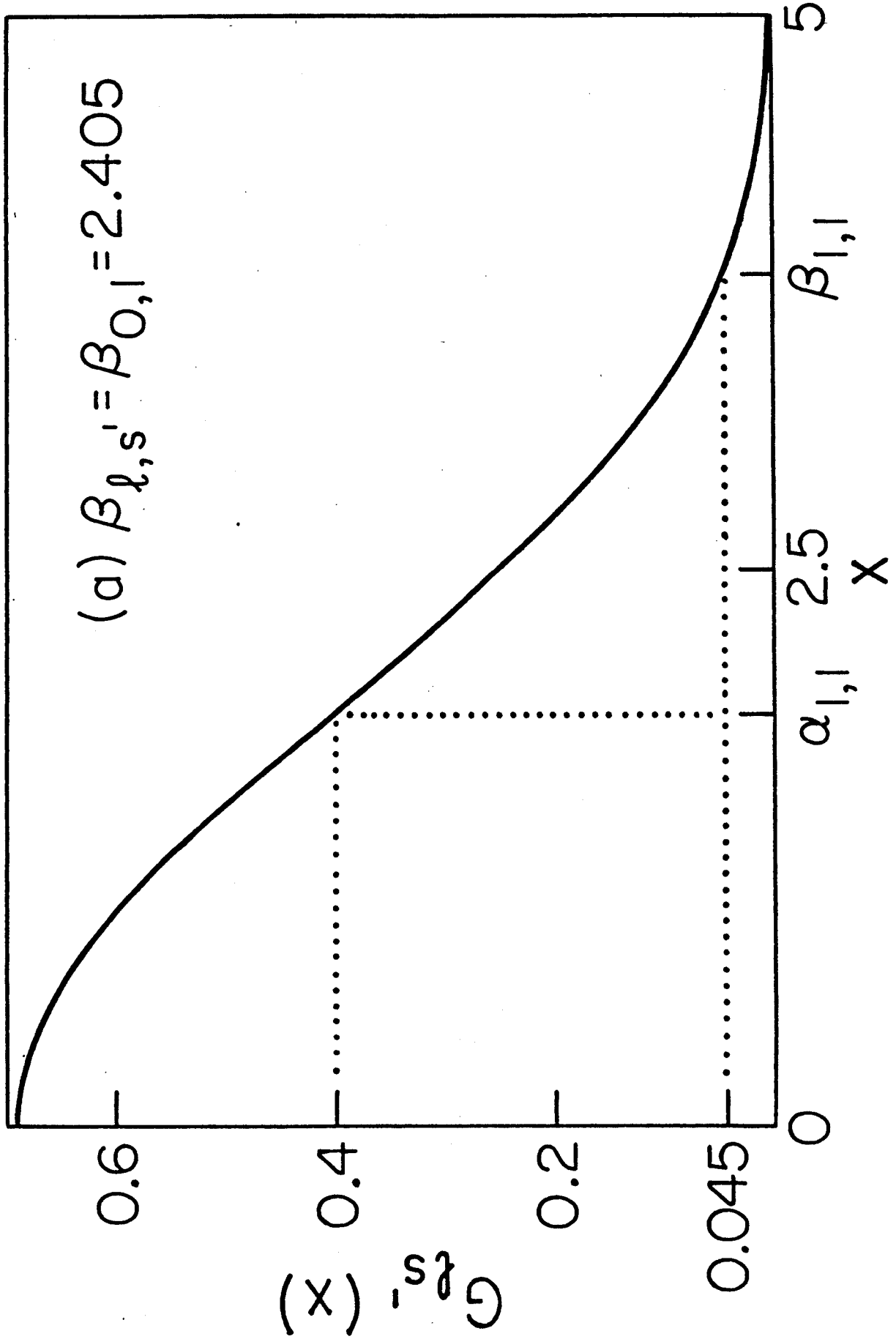
(a) $\beta_{\ell,s'} = \beta_{0,1} = 2.405$
$G_{\ell s'}(x)$
0.6
0.4
0.2
0.045
0
2.5
5
x
$\alpha_{1,1}$
$\beta_{1,1}$

Fig. 1(a)

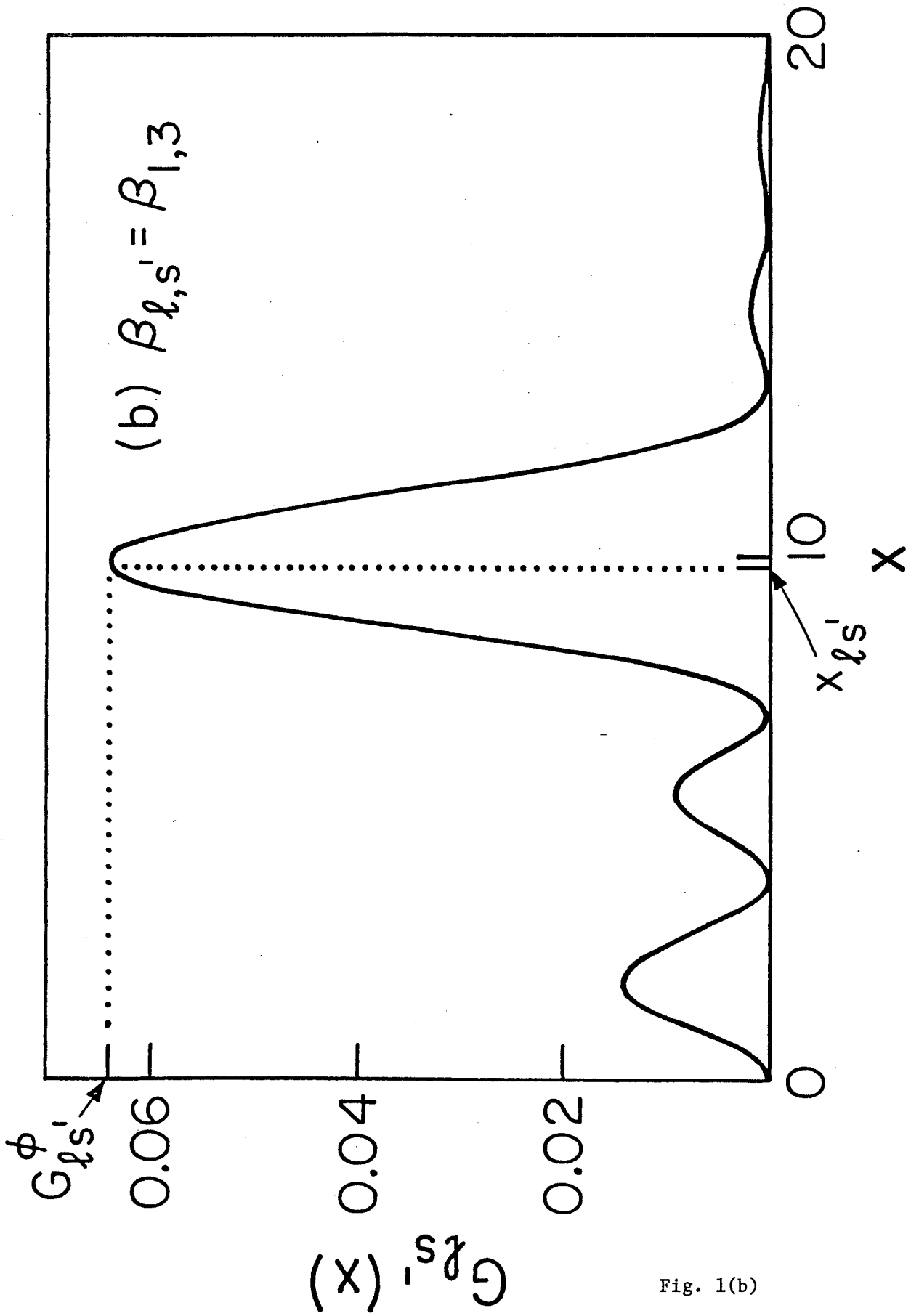

Fig. 1(b)

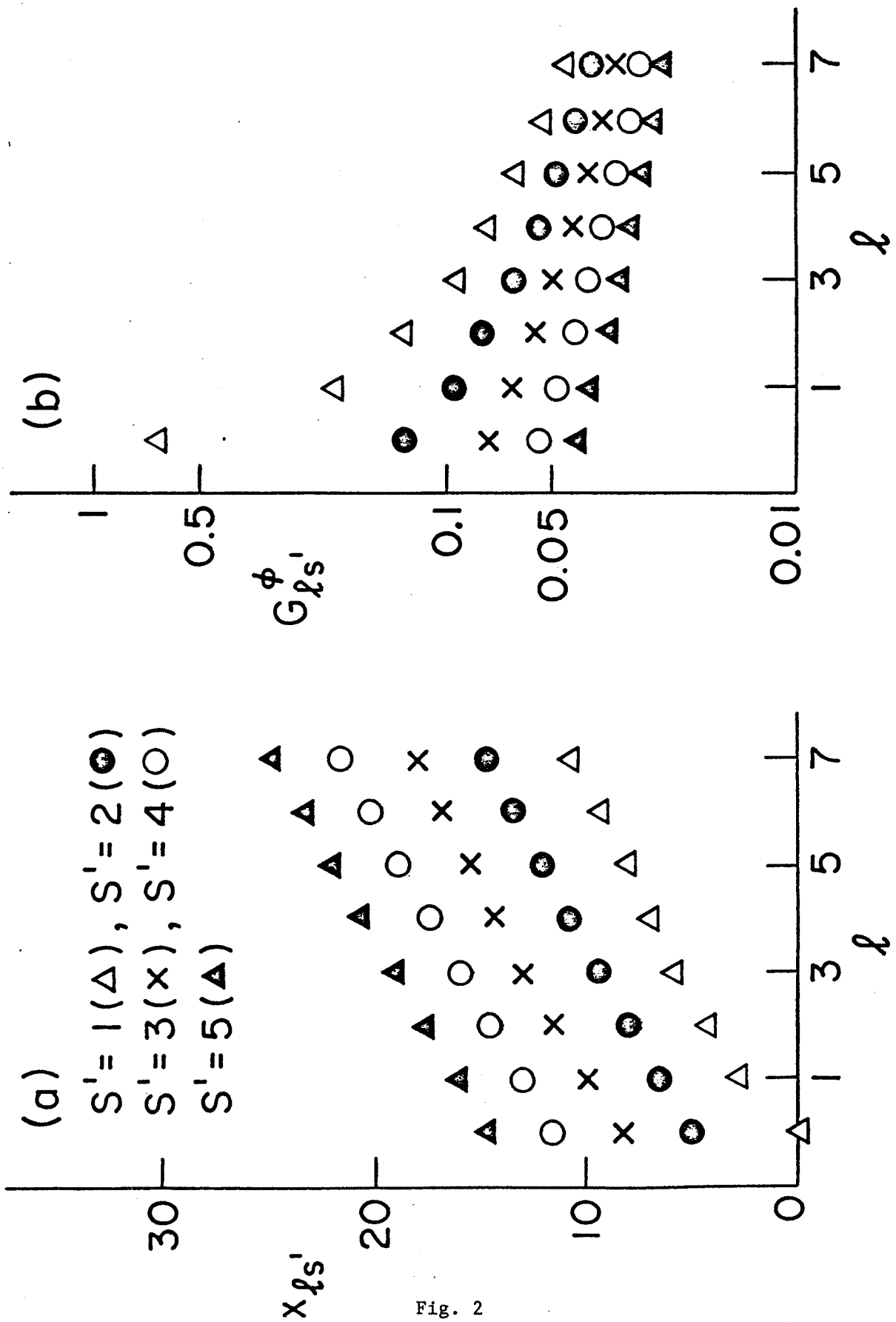
(a)
S'= 1 (△), S'= 2 (●)
S'= 3 (×), S'= 4 (○)
S'= 5 (▲)
$x_{\ell s'}$
30
20
10
0
1
3
5
7
ℓ
(b)
$G^{\phi}_{\ell s'}$
1
0.5
0.1
0.05
0.01
1
3
5
7
ℓ

Fig. 2

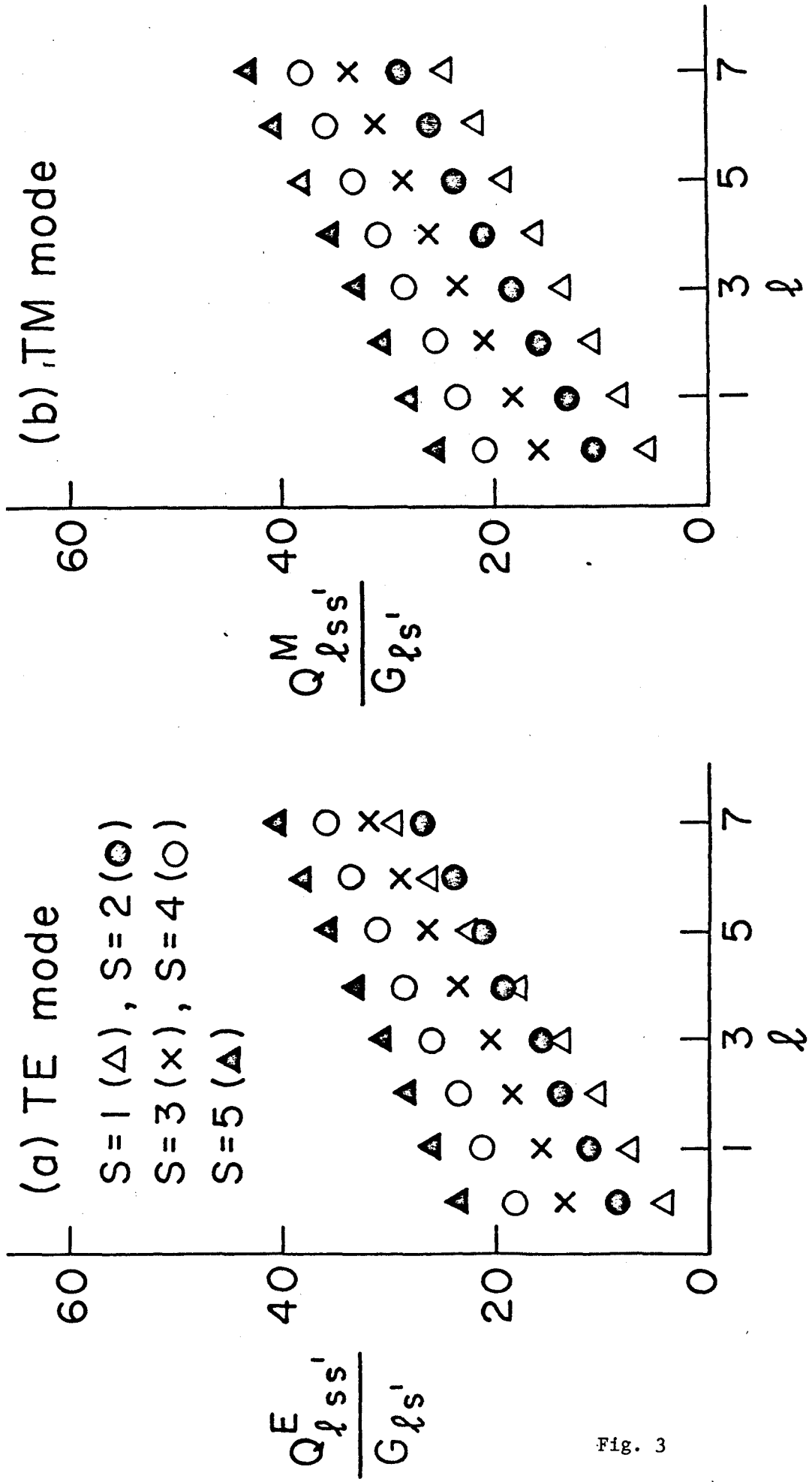
(a) TE mode
S=1 (Δ), S=2 (●)
S=3 (×), S=4 (○)
S=5 (▲)
$Q^E_{\ell ss'} / G_{\ell s'}$
60
40
20
0
1
3
5
7
ℓ
(b) TM mode
$Q^M_{\ell ss'} / G_{\ell s'}$
60
40
20
0
1
3
5
7
ℓ

Fig. 3

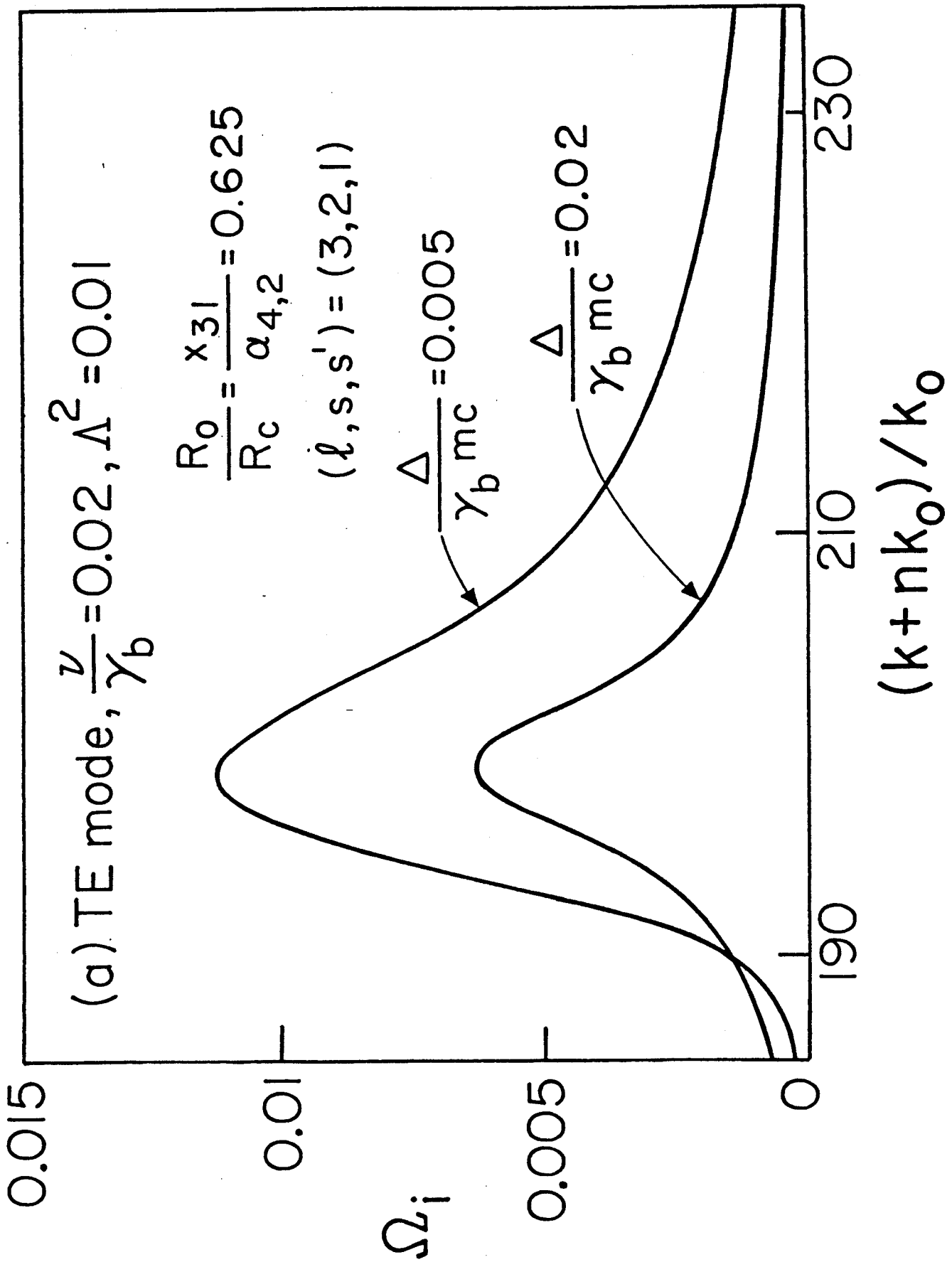
(a) TE mode, $\frac{\nu}{\gamma_b}=0.02, \Lambda^2=0.01$
$\frac{R_o}{R_c}=\frac{x_{31}}{\alpha_{4,2}}=0.625$
$(\ell, s, s') = (3,2,1)$
$\frac{\Delta}{\gamma_b mc}=0.005$
$\frac{\Delta}{\gamma_b mc}=0.02$
Ω_i
0.015
0.01
0.005
0
190
210
230
$(k+nk_o)/k_o$

Fig. 4(a)

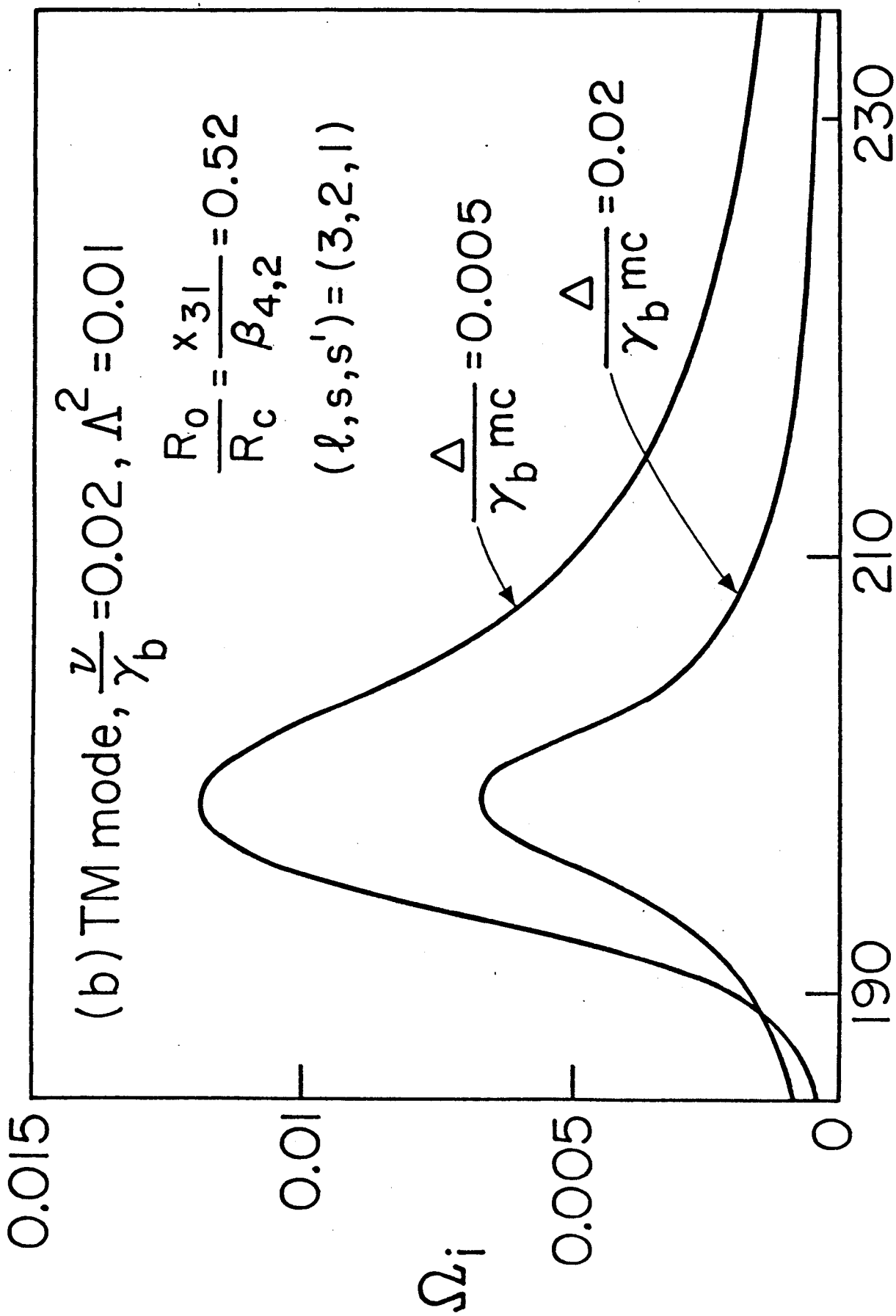
(b) TM mode, $\frac{\nu}{\gamma_b}=0.02$, $\Delta^2=0.01$
$\frac{R_0}{R_c}=\frac{x_{31}}{\beta_{4,2}}=0.52$
$(\ell,s,s')=(3,2,1)$
$\frac{\Delta}{\gamma_b mc}=0.005$
$\frac{\Delta}{\gamma_b mc}=0.02$
Ω_i
0.015
0.01
0.005
0
190
210
230
$(k+nk_0)/k_0$

Fig. 4(b)